

Article

# Optimal Energy Management of Combined Cooling, Heat and Power in Different Demand Type Buildings Considering Seasonal Demand Variations

Akhtar Hussain <sup>1</sup>, Van-Hai Bui <sup>1</sup>, Hak-Man Kim <sup>1,\*</sup>, Yong-Hoon Im <sup>2</sup> and Jae-Yong Lee <sup>2,\*</sup>

<sup>1</sup> Department of Electrical Engineering, Incheon National University, 12-1 Songdo-dong, Yeonsu-gu, Incheon 406840, Korea; hussainakhtar@inu.ac.kr (A.H.); buivanhaibk@inu.ac.kr (V.-H.B.)

<sup>2</sup> Korea Institute of Energy Research, 152 Gajeong-ro, Yuseong-gu, Daejeon 34129, Korea; iyh@kier.re.kr

\* Correspondence: hmkim@inu.ac.kr (H.-M.K.); jylee@kier.re.kr (J.-Y.L.); Tel.: +82-32-835-8769 (H.-M.K.); Fax: +82-32-835-0773 (H.-M.K.)

Academic Editors: Yacine Rezgui and Monjur Mourshed

Received: 28 March 2017; Accepted: 3 June 2017; Published: 8 June 2017

**Abstract:** In this paper, an optimal energy management strategy for a cooperative multi-microgrid system with combined cooling, heat and power (CCHP) is proposed and has been verified for a test case of building microgrids (BMGs). Three different demand types of buildings are considered and the BMGs are assumed to be equipped with their own combined heat and power (CHP) generators. In addition, the BMGs are also connected to an external energy network (EEN), which contains a large CHP, an adsorption chiller (ADC), a thermal storage tank, and an electric heat pump (EHP). By trading the excess electricity and heat energy with the utility grid and EEN, each BMG can fulfill its energy demands. Seasonal energy demand variations have been evaluated by selecting a representative day for the two extreme seasons (summer and winter) of the year, among the real profiles of year-round data on electricity, heating, and cooling usage of all the three selected buildings. Especially, the thermal energy management aspect is emphasized where, bi-lateral heat trading between the energy supplier and the consumers, so-called energy prosumer concept, has been realized. An optimization model based on mixed integer linear programming has been developed for minimizing the daily operation cost of the EEN while fulfilling the energy demands of the BMGs. Simulation results have demonstrated the effectiveness of the proposed strategy.

**Keywords:** building microgrids (BMGs); energy management; energy prosumer; microgrid operation; combined cooling; heat and power; thermal energy storage

## 1. Introduction

Microgrid penetration has increased at medium and low voltage levels in developed/developing countries worldwide. One major economic potential of microgrids with various distributed generators is the local utilization of waste heat generated during the conversion of primary fuel to electricity [1]. Various types of distributed generators along with small-scale combined heat and power (CHP) and combined cooling, heat and power (CCHP) equipment are used for district heating and/or cooling. Dispatchability and higher efficiency of total energy along with economic and environmental benefits make CHP/CCHP systems of particular value to microgrids [2]. About 30% of the fuel's available energy is converted to usable energy (electricity) by conventional power plants. Microgrids with CCHP systems can utilize 75–80% of fuel source [3,4]. Public buildings like residential apartments, commercial buildings, schools, hospitals, universities, and parks with their own local CHP generations form a major portion of CCHP microgrids. According to energy information administration (EIA), 48% of the energy used in buildings is for heating and cooling purposes [5]. Integration of renewable

and energy efficient technologies have increased in public buildings in Korea also, due to the recent obligations to obtain 10% of their total energy consumption from new and renewable energy sources [6]. The term building microgrid (BMG) has been used in this paper to address those public buildings, which have both local energy sources and demands (electrical and thermal).

Future energy systems are predicted to be comprised of multiple microgrids, which can trade energy among themselves as well as with the utility grid [7]. In order to deploy multi-microgrids on a large scale, the design, architecture, and operation of these systems are required to be cost effective, efficient, environment-friendly, and reliable. Various studies have been conducted for scheduling the resources of microgrids/multi-microgrids, which are named as BMGs in this paper. Both CHP systems (bi-generation systems) [8–15], and CCHP systems (tri-generation systems) [16–24] have been analyzed in different studies.

An experimental power grid center has been described in [8] for developing and testing the CHP technologies for microgrids. Optimal operation of CHP systems based on real-time market prices along with varying ratio between heat and electricity outputs of CHPs has been analyzed by Gu et al. [9]. Temperature dynamics of district heating network have been considered in [10] for the dispatch of CHP systems while, in [11], district heating network dynamics have been analyzed for unit-commitment of CHP systems considering energy transmission constraints. A generalized approach for assessing the mutual (heat and power) impacts of CHP-based distributed generators has been proposed by Zhang et al. [12]. Planning-stage optimization for CHP systems has been proposed by Negendahl et al. [13] and economic dispatch has been studied in [14]. A sequentially coordinated energy management strategy has been proposed in [15] for scheduling CHPs and heat only boilers for multi-microgrid systems. In [16], global optimization has been achieved by coordinating information between local energy management systems and the central energy management system.

A microgrid central controller has been used for scheduling the dispatchable CCHP plants in both day-ahead and real-time scheduling horizons by Bracco et al. [16]. A method for optimizing the energy (electricity, heat, and cooling) generation and usage in urban areas has been proposed by Ascione et al. [17] and has been tested in a southern Italian city. A two-stage optimal algorithm for CCHP microgrids from a design and planning perspective has been proposed by Guo et al. [18]. Siting and sizing of tri-generation equipment for CCHP microgrids considering uncertainties are proposed by Hussain et al. [19]. A comprehensive review has been carried out by Gu et al. [20] on planning, scheduling, and control of CCHP systems. Different algorithms for optimization of CCHP systems have been proposed in [21,22]. The authors in [23] have considered the integration of electrical vehicles while the authors in [22] have considered the reliability of the microgrids. A study has been conducted in [23] regarding the usage of wastes for CCHP applications. Both energy matching and optimization aspects of CCHP systems have been considered by the authors. Economic impacts of converting conventional power stations to CCHPs have been analyzed in [24,25].

Recently, artificial intelligence techniques for the operation of smart grids/microgrids have also gained popularity. In [26], distributed constraint optimization problems (DCOPs) have been solved by using off-the-shelf DCOP algorithms. Adaptive learning methods have been used in [27,28] for energy management of buildings in a multi-agent environment. Multi-agent-based systems have been used for the autonomous operation of smart buildings and homes in [29–31]. Consensus and distributed gradient algorithms are used by Zhang et al. [32] and a fully distributed solution is proposed for the operation of smart grids.

Most of the studies available in the literature on the scheduling of microgrid CCHP systems [16–24] are concentrated on a single microgrid. However, in order to benefit from microgrids, networking of various microgrids to form a multi-microgrid system has emerged in the literature as an advanced form and application of the microgrid concept [33,34]. This interconnection may result in scheduling issues, especially if the microgrids lie within the same metrological locality (which is commonly practiced). A feasible solution for multi-microgrids having CCHP systems is more challenging and desirable than for single microgrids [33].

In this paper, a mathematical model based on mixed integer linear programming has been formulated for managing all the three forms of energies for BMGs in the proposed building multi-microgrid system. The proposed building multi-microgrid system comprises of three different demand types of buildings with their own local CHP generations: BMGs, and an external energy network (EEN) having a large CHP, adsorption chiller (ADC), thermal storage tank, and electric heat pump (EHP). The objective of the developed model is to minimize the operation cost of EEN while fulfilling the CCHP needs of BMGs in the building multi-microgrids system. This will result in bi-lateral heat trading between the conventional energy supplier and the consumers resulting in the involvement of energy prosumer stakeholders. In order to cater the seasonal variations in energy demands of BMGs, representative days have been selected for the two extreme seasons of the year. 15th of July and 15th of January have been taken as representative days for summer and winter seasons, respectively. Three different buildings have been selected in Seoul (Korea) and their demand profiles have been monitored throughout the year. The CCHP demand profiles of these buildings have been used for the simulations. The major contributions of this study can be summarized as follows:

- In contrast to the existing literature, where direct networking of microgrids is considered, networking of microgrids via an EEN is proposed. This indirect networking can benefit the network in following ways:
  - (a) Bi-lateral heat trading between the energy supplier and the consumers, so-called energy prosumer concept, can be realized for reducing losses of the network.
  - (b) During the summer season, surplus heat can be sold to the EEN, which is utilized by EEN for fulfilling the cooling demand of the network, i.e., reduced operation cost of the network.
  - (c) Due to cooling networking, individual BMGs do not need to install local cooling devices, which results in the reduction of investment cost.
- Apart from above-mentioned contributions, real load profiles of different demand type buildings have been used for evaluating seasonal energy demand variations. Additionally, all the formulations are based on mixed integer linear programming, which are easy to implement.

## 2. System Configuration

Various energy management strategies have been used in the literature for scheduling microgrids/multi-microgrids [10–25]. Among those, the cooperative multi-microgrid community has gained popularity due to its merits like minimum operation cost of the entire network, network level resource-aware optimization, better utilization of efficient units of individual microgrids, etc. Therefore, this paper also utilizes the concept of cooperative multi-microgrid community for realizing the proposed optimization approach.

A cooperative network of three different demand type building microgrids (BMG1, BMG2, and BMG3) with an external thermal energy provider company has been considered in this study. Figure 1 shows the schematic diagram of the building multi-microgrid system considered in this study. Each BMG contains a small CHP along with electricity, heating, and cooling demands. BMG1 is an apartment complex (residential building), BMG2 is a complex mall (commercial building), and BMG3 is an office (industrial building). A Stirling engine has been used in BMG1, fuel cell in BMG2, and steam turbine in BMG3 as CHP units of individual BMGs. The large CHP in the EEN is also equipped with a gas turbine or a gas engine. In order to ensure the energy supply reliability to the customers during the whole year, EEN has been proposed in this paper as highlighted in Figure 1 with color. The large CHP, EHP, ADC, thermal storage tank, and thermal energy network (heating and cooling) are assumed to belong to the EEN.

Each BMG can fulfill its electric load demand by either using its CHP unit or by trading with the utility grid. Similarly, heat energy demand can be fulfilled by either using the local CHP or by trading with the EEN (thermal storage tank) as shown in Figure 2a. EHP and ADC are used for fulfilling the

cooling demands of the BMGs as shown in Figure 2b. Due to the presence of cooling network, BMGs are not required to be equipped with local cooling devices to avoid overlapped investment cost and for better utilization of space for it. Energy from large CHP can be used for fulfilling the heat demands of BMGs when small CHPs of respective BMGs are not able to fulfill their heat demand. The electricity generated by large CHP can either be used by the EHP or can be sold to the utility grid. Similarly, the heat energy of large CHP can be used either for ADC or for charging thermal storage tank as shown in Figure 2c. Excess of thermal energy from BMGs can be sold to the EEN and shortage amount can be bought from the EEN (thermal storage tank) as shown in Figure 2d.

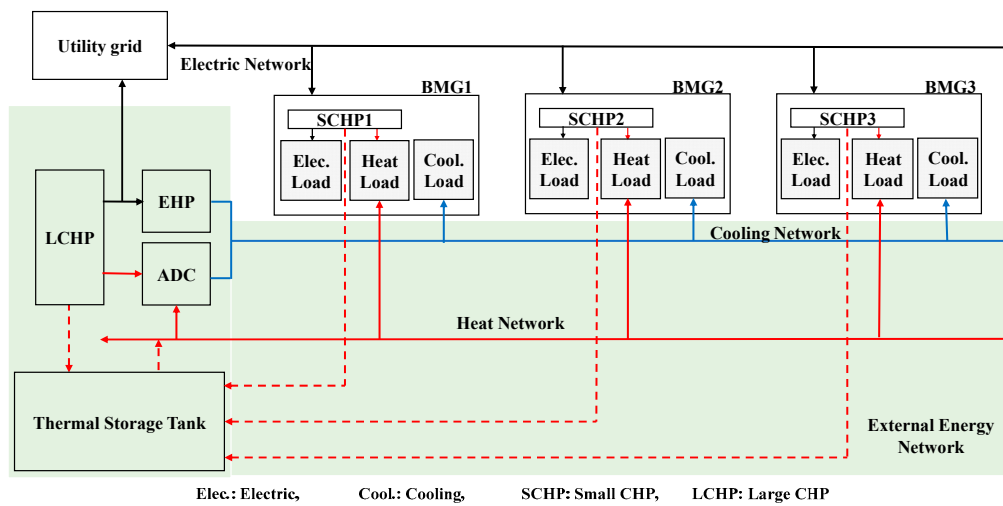


Figure 1. Schematic diagram of electricity, heating, and cooling networks in the proposed system.

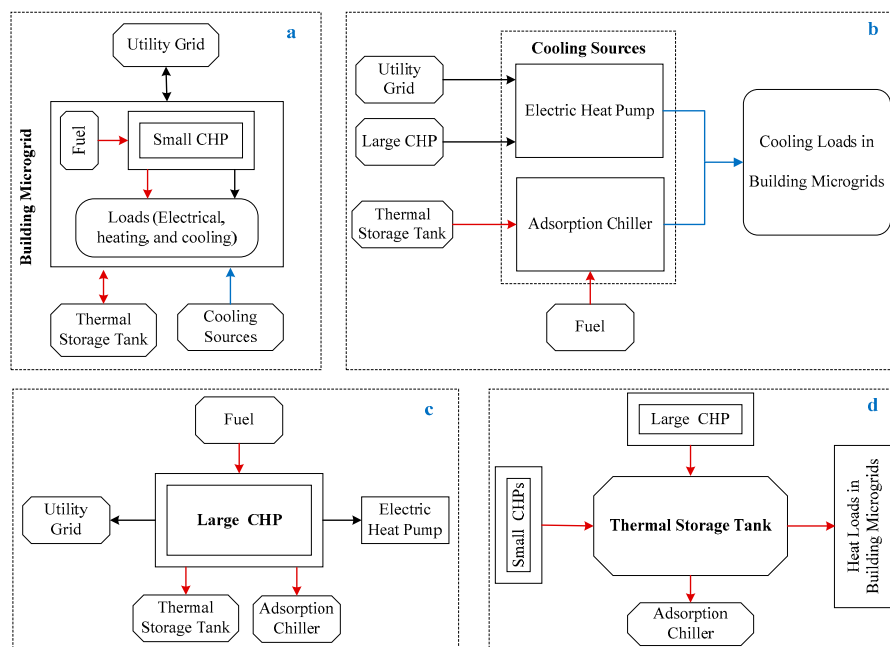


Figure 2. Energy balancing in the proposed multi-microgrid system: (a) CCHP in individual BMGs; (b) cooling energy; (c) large CHP; and (d) thermal storage tank.

ADC uses the heat stored in the thermal storage tank first, and in the case of heat shortage, the large CHP is operated by EEN to supply the required amount of heat for ADC. The price of selling excess heat energy to the EEN is different for different BMGs and it also varies with seasons of the year, even for the same BMG. Heat energy will be wasted only when there is no remaining capacity in

the thermal storage tank for storing (fully charged) the heat energy. Comparative analysis of different open and closed-cycle heat engines (used in this paper) for small CHPs usage has been carried out by Nguyen et al. [34] and different chillers have been analyzed by Underwood et al. [35].

The operating temperature of the suggested network is assumed to be around 65 °C, which is slightly higher than those of low-temperature district heating network, so-called “4th generation district heating systems”. This is due to the presence of cooling network in the proposed energy management strategy and utilization of ADC for generation of cooling energy. The cooling network has been considered for efficient utilization of the waste heat from the buildings connected to the heating grid. The details of low heating distribution networks along with technical issues and proposed solutions can be found in [36].

### 3. Problem Formulation

In this section, a mixed integer linear programming-based model has been developed for scheduling of the proposed building multi-microgrid system. The proposed model is formulated for a 24-h scheduling horizon with a time interval of  $t$ , which could be any uniform interval of time. However, in the proposed scheduling, it has been assumed as 1 h. All the data from EEN and BMGs will be directed to the building energy management system. Building energy management system will perform optimization and inform each component about its scheduling.

The load profiles of individual BMGs for different seasons of the year and market price signals (buying and selling prices) of the utility grid are taken as inputs. In addition, the price for trading heat energy by individual BMGs with the EEN and price of buying cooling energy from the EEN are also assumed to be known for different seasons of the years. The objective of this formulation is to minimize the operation cost of the network while respecting some equality and inequality constraints related to the above-mentioned variables. The output of this formulation is the optimal values of the above-mentioned variables for different set of input parameters.

#### 3.1. Objective Function

The cost function of the network is the total expenses occurred for the EEN when external trading of electricity and internal trading of heat are applied as given by Equation (1). Let  $E^{EEN} = C_{EEN}(P_{CHP}^L(t), P_{BUY}^e(t), P_{SELL}^e(t), Q_{DISCH}^h(t), Q_{CH}^h(t), Q_{ADC}^c(t), Q_{EHP}^c(t))$  be the set of control variables for deciding the operation cost of the network. Then, the objective of the formulation is to minimize the overall cost of the network as given by Equation (2):

$$\begin{aligned}
 C_{EEN}(P_{CHP}^L(t), P_{BUY}^e(t), P_{SELL}^e(t), Q_{DISCH}^h(t), Q_{CH}^h(t), Q_{ADC}^c(t), Q_{EHP}^c(t)) = & \\
 \sum_{t=1}^T (C_{CHP}^L \cdot P_{CHP}^L(t) + y_L(t) \cdot SUC_{CHP}^L(t)) + \sum_{t=1}^T (PR_{BUY}^e(t) \cdot P_{BUY}^e(t) - PR_{SELL}^e(t) \cdot P_{SELL}^e(t)) & \\
 + \sum_{t=1}^T (C_{ADC} \cdot Q_{ADC}^c(t) + y_a(t) \cdot SUC_{ADC}(t)) & \\
 - \sum_{t=1}^T \sum_{m=1}^M (PR_{SELL}^h(t) \cdot Q_{DISCH}^h(t) - PR_{BUY}^h(t) \cdot Q_{CH}^h(t)) & \\
 - \sum_{t=1}^T \sum_{m=1}^M (PR_{SELL}^c(t) \cdot (Q_{ADC}^c(t) + Q_{EHP}^c(t))) &
 \end{aligned} \tag{1}$$

$$\begin{aligned}
 Let E^{EEN} = C_{EEN}(P_{CHP}^L(t), P_{BUY}^e(t), P_{SELL}^e(t), Q_{DISCH}^h(t), Q_{CH}^h(t), Q_{ADC}^c(t), Q_{EHP}^c(t)) & \\
 E^{EEN*}(t) = \arg \min \{C_{EEN}(E^{EEN})\} &
 \end{aligned} \tag{2}$$

The first term in Equation (1) shows the generation cost of large CHP along with its startup cost. The second term shows the price for buying and selling electricity from/to the utility grid by the EEN. The third term shows the generation and startup costs of the ADC unit in EEN. The fourth term shows the price for selling and buying heat energy to/from the BMGs. The last term shows the profit gained

by selling cooling energy to BMGs. The total energy optimization function when external trading of electric energy with the utility grid and internal trading of thermal energy with the BMGs are applied can be expressed by using Equation (2).

$$\begin{aligned} & \sum_{t=1}^T \sum_{k=1}^K \left( x_{k,m} \cdot C_{k,m}^s \cdot P_{k,m}^s(t) + y_{k,m}(t) \cdot SUC_{k,m}^s(t) \right) + \sum_{t=1}^T \left( PR_{BUY}^e(t) \cdot P_{BUY_m}^s(t) - PR_{SELL}^e(t) \cdot P_{BUY_m}^s(t) \right) \\ & + \sum_{t=1}^T \left( PR_{BUY_m}^h(t) \cdot Q_{DISCH_m}^h(t) - PR_{SELL_m}^h(t) \cdot Q_{CH_m}^h(t) \right) + \sum_{t=1}^T \left( PR_{SELL_m}^c(t) \cdot (Q_{ADC}^c(t) + Q_{EHP}^c(t)) \right) \end{aligned} \quad (3)$$

where:

$$\sum_{k=1}^K x_{k,m} = 1, \quad x_{k,m} \in \{0, 1\}, \quad \forall k, m \quad (4)$$

The objective of individual BMGs is to minimize their respective operation costs as given by (3). The first term in Equation (3) shows the operation and startup costs of small CHP units in the  $m$ th microgrid. The second term shows the price for buying and selling electricity from/to the utility grid by  $m$ th microgrid. The third term shows the price for selling and buying heat energy to/from the EEN by  $m$ th microgrid. The last term shows the price for buying cooling energy from the EEN by  $m$ th microgrid. Equation (4) implies that each BMG contains one of the three small CHPs, i.e., Stirling engine, fuel cell, and gas turbine. In  $x_{k,m}$ ,  $k$  indicates the presence of one of these small CHP units in different BMGs. BMG1 contains a Stirling engine ( $k = 1$ ), BMG2 contains a fuel cell ( $k = 2$ ), and BMG3 contains a gas turbine ( $k = 3$ ). Therefore, the objective function of the individual BMGs contains the cost for operation of their respective small CHP units, as shown in Equation (3).

### 3.2. Load Balancing Constraints

EHP, ADC, large CHP, and thermal storage tank are assumed to be owned by a single stakeholder, which is named as EEN in this paper. Therefore, heat energy of large CHP will be charged to the thermal storage tank (free of cost). The amount of charging will be constrained by the capacity of the thermal storage tank. Similarly, the amount of heat energy required for ADC will be discharged from the thermal storage tank (free of cost). The dischargeable amount will be limited by the heat storage tank's heat content of storage (HCS) of the previous time step. Throughout the paper, HCS is used to indicate the amount of thermal energy present in the tank, i.e., analogous to state-of-charge for battery energy storage systems. As mentioned earlier, the owner of large CHP, ADC, EHP, and storage tank is assumed same. Therefore, charging of thermal energy to the storage tank by the large CHP and discharging of thermal energy by ADC from the storage tank will not involve energy-trading cost, i.e., free of cost:

$$P_{LOAD_m}^e(t) = \sum_{k=1}^K \left( x_{k,m} \cdot P_{k,m}^s(t) \right) + \left( 1 - P_{loss_m}^s \right) \cdot P_{BUY_m}^s(t) - P_{SELL_m}^s(t) / \left( 1 - P_{loss_m}^s \right), \quad \forall m, k, t \quad (5)$$

$$P_{EHP}^e(t) = P_{CHP}^L(t) + \left( 1 - P_{loss}^L \right) \cdot P_{BUY_L}^e(t) - P_{SELL_L}^e(t) / \left( 1 - P_{loss}^L \right), \quad \forall t \quad (6)$$

$$Q_{LOAD_m}^h(t) = \left( x_{k,m} \cdot Q_{k,m}^h(t) \right) + \left( 1 - Q_{loss_m}^h \right) \cdot Q_{DISCH_m}^h(t) - Q_{CH_m}^h(t) / \left( 1 - Q_{loss_m}^h \right) + Q_{W_m}^h(t), \quad \forall m, k, t \quad (7)$$

$$Q_{LOAD_m}^c(t) = \left( 1 - Q_{loss_m}^c \right) \cdot \left( Q_{ADC_m}^c(t) + Q_{EHP_m}^c(t) \right), \quad \forall m, t \quad (8)$$

$$Q_L^h(t) = \left( 1 - Q_{loss}^h \right) \cdot Q_{LCH}^h(t) + Q_{EW}^h(t), \quad \forall t \quad (9)$$

The electricity demand in each BMG can be fulfilled either by using the electricity generated by the local small CHP or by buying from the utility grid. Excess of electric energy can be sold to the utility grid by each BMG as given by Equation (5). The line losses occurred due to trading of electricity between the  $m$ th BMG and the utility grid is modeled as  $P_{loss_m}^s$ . The value of  $P_{loss_m}^s$  could be between zero and one, where higher value of  $P_{loss_m}^s$  indicates lines with higher losses. The amount of electricity generated by the large CHP is primarily used for operating the EHP. However, excess electricity can be sold to the utility grid. If the amount of electricity generated by the large CHP is not sufficient for EHP,

EEN can buy the required amount of electricity from the utility grid as given by Equation (6). Similarly, the line losses introduced due to trading of electricity between the EEN and the utility grid is modeled as  $P_{loss}^L$  where,  $P_{loss}^L \in [0, 1]$ . Heat demand in each BMG can be fulfilled by either using the heat energy generated by the local small CHP or by buying from the EEN while the excess of heat energy can be sold to the EEN as shown in Equation (7). During trading of thermal energy between BMGs and the EEN, some of the energy will be wasted as pipelines losses, which is modeled as  $Q_{loss_m}^h$ . Similarly, the pipeline losses of the pipe connecting large CHP and the storage tank of EEN is modeled as  $Q_{loss}^h$ . Therefore,  $1 - Q_{loss_m}^c$  and  $1 - Q_{loss}^h$  indicate the efficiencies of the respective pipelines. Thermal energy will be wasted only when the thermal storage tank is fully charged. The cooling demand in each BMG can be fulfilled by buying cooling energy from the EEN. EEN may use ADC and/or EHP for generating cooling energy as given by Equation (8). Similar to heat energy, some of the cooling energy will be wasted as pipeline losses during transporting it from the EEN to BMGs, which is modeled as  $Q_{loss_m}^c$ , where  $Q_{loss_m}^c \in [0, 1]$ .

$$Q_W^h(t) = \sum_{m=1}^M Q_{W_m}^h(t) + Q_{EW}^h(t), \forall m, t \quad (10)$$

$$Q_{EHP}^c(t) = \sum_{m=1}^M Q_{EHP_m}^c(t), Q_{ADC}^c(t) = \sum_{m=1}^M Q_{ADC_m}^c(t), \forall m, t \quad (11)$$

$$Q_{CH}^h(t) = \sum_{m=1}^M (1 - Q_{loss_m}^h) \cdot Q_{CH_m}^h(t) + (1 - Q_{loss}^h) \cdot Q_{LCH}^h(t), \forall m, t \quad (12)$$

$$Q_{DISCH}^h(t) = \sum_{m=1}^M Q_{DISCH_m}^h(t) / (1 - Q_{loss_m}^h) + Q_{ADC}^h(t) / (1 - Q_{loss}^h), \forall m, t \quad (13)$$

$$P_{BUY}^e(t) = \sum_{m=1}^M (1 - P_{loss_m}^s) \cdot P_{BUY_m}^s(t) + (1 - P_{loss}^L) \cdot P_{BUY_L}^e(t), \forall m, t \quad (14)$$

$$P_{SELL}^e(t) = \frac{\sum_{m=1}^M \frac{P_{SELL_m}^s(t)}{(1 - P_{loss_m}^s)} + P_{SELL_L}^e(t)}{(1 - P_{loss}^L)}, \forall m, t \quad (15)$$

Large CHP may also have to waste heat energy when the storage tank is fully charged. Heat energy balancing of large CHP is given by Equation (9). The total amount of thermal energy wasted at any time interval  $t$  can be calculated by summing the wasted energy of individual BMGs and that of EEN considering thermal energy losses, as given by Equation (10). The amount of cooling energy generated by EHP should be balanced by the total amount of cooling energy used by individual BMGs from the EHP along with pipe losses as given by Equation (11). Same is the case with ADC as shown in Equation (11). The total amount of thermal energy charged to the thermal storage tank at any time interval  $t$  can be calculated by summing the amount of thermal energy sold by individual BMGs and amount of heat energy charged by large CHP, as shown in Equation (12). The thermal storage tank can be discharged for fulfilling the heat energy demands of individual BMGs and/or can be used for converting heat energy to cooling energy by EEN as shown in Equation (13). During charging and discharging of heat to/from the storage tank, the efficiencies of pipes ( $1 - Q_{loss_m}^h$ ) connecting BMGs with the storage tank are considered as given by Equations (12) and (13). Similarly, during trading power between the  $m$ th BMG and the utility grid, efficiency of line connecting that BMG with the utility grid is considered, as given by Equations (14) and (15). The total amount of electricity traded by the entire building multi-microgrid system with the utility grid can be calculated by using Equations (14) and (15).

### 3.3. Generation Constraints

Generation limits for CHPs, EHP, and ADC in the building multi-microgrid system are as follows:

$$u_{k,m}(t) \cdot \min [P_{k,m}^e(t)] \leq P_{k,m}^e(t) \leq \max [P_{k,m}^e(t)] \cdot u_{k,m}(t), \forall k, m, t \quad (16)$$

$$u_L(t) \cdot \min[P_L^e(t)] \leq P_L^e(t) \leq \max[P_L^e(t)] \cdot u_L(t), \forall t \quad (17)$$

$$\min[P_{EHP}^e(t)] \leq P_{EHP}^e(t) \leq \max[P_{EHP}^e(t)], \forall t \quad (18)$$

$$u_a(t) \cdot \min[Q_{ADS}^c(t)] \leq Q_{ADS}^c(t) \leq \max[Q_{ADS}^c(t)] \cdot u_a(t), \forall t \quad (19)$$

The generation constraint for small CHP units is given by Equation (16). Where  $k$  indicates the type of small CHP in each BMG. The frequent switching between on and off modes of these units is controlled by the startup cost ( $y_{k,m}(t) \cdot SUC_{k,m}^u(t)$ ), mentioned in Equation (3). All the small CHPs can operate between their specified minimum and maximum operation ranges, as given by Equation (16). The constraints for large CHP in EEN is given by Equation (17). Equations (18) and (19) show the operation ranges for EHP and ADC, respectively:

$$y_{k,m}(t) = \max\{(u_{k,m}(t) - u_{k,m}(t-1)), 0\}, \forall m, k, t \quad (20)$$

$$y_L(t) = \max\{(u_L(t) - u_L(t-1)), 0\}, \forall t \quad (21)$$

$$y_a(t) = \max\{(u_a(t) - u_a(t-1)), 0\}, \forall t \quad (22)$$

$$u_{k,m}(t), u_L(t), u_a(t) \in \{0, 1\}, \forall m, k, t \quad (23)$$

$y_{k,m}(t)$  in Equation (20) is the startup indicator for each small CHP in the  $m$ th BMG. This indicator will take the value of 1 when  $(u_{k,m}(t) - u_{k,m}(t-1)) > 0$  otherwise, it will be zero. Same is the case with startup indicator of large CHP and ADC as given by Equations (21) and (22), respectively. Equation (23) shows that commitment status indicators ( $u_{k,m}(t)$ ,  $u_L(t)$ , and  $u_a(t)$ ) of small CHPs, large CHP, and ADC are binary variables and can take either 1 or 0 value at each time interval  $t$ .

### 3.4. Heat to Power Ratio and Energy Efficiency Ratings

Heat to power ratio of different CHP generation units and energy efficiency ratings of different cooling energy generators used in this study are given by following equations:

$$Q_{k,m}^h(t) = P_{k,m}^s(t) \cdot \eta_{k,m}, \forall m, k, t \quad (24)$$

$$Q_L^h(t) = P_{CHP}^L(t) \cdot \eta_L, \forall t \quad (25)$$

$$\min[\eta_{k,m}] \leq \eta_{k,m}(t) \leq \max[\eta_{k,m}], \forall m, k, t \quad (26)$$

$$\min[\eta_L] \leq \eta_L(t) \leq \max[\eta_L], \forall t \quad (27)$$

$$Q_{ADC}^c(t) = Q_{ADC}^h(t) \cdot \eta_{ADC}, \forall t \quad (28)$$

$$Q_{EHP}^c(t) = P_{EHP}^e(t) \cdot \eta_{EHP}, \forall t \quad (29)$$

Equation (24) shows the heat to power ratio of  $k$ th small CHP in  $m$ th BMG. Similarly, Equation (25) shows the heat to power ratio of large CHP in EEN. The limits of heat to power ratios for small CHPs are constrained by Equation (26) and that of large CHP by Equation (27). In order to enhance the lifetime of CHPs, these values ( $\eta_{k,m}$  and  $\eta_L$ ) are not altered on daily basis. Equations (28) and (29) shows energy efficiency ratings of ADC and EHP, respectively. These values ( $\eta_{ADC}$  and  $\eta_{EHP}$ ) being equipment specific, have been taken as same for all the seasons.

### 3.5. Thermal Storage Tank Constraints

It can be observed from Equations (30)–(34) that the charging, discharging, and HCS calculations at each time interval  $t$  require the HCS information of previous time interval, i.e., time interval  $t - 1$ . Therefore, the value of  $HCS(t - 1)$  at the first interval will be replaced with the initial value of thermal energy in thermal storage tank, i.e.,  $SQ_{TST}^{INI}$ . The charging and discharging amount of energy from thermal storage tank are constrained by Equations (30) and (31), respectively. The HCS of thermal

storage tank at each time interval depends upon the amount of thermal energy added at time interval  $t$ , amount of thermal energy taken from thermal storage tank at time interval  $t$ , and HCS of time interval  $t - 1$  as given by Equation (32). The HCS at each time interval  $t$  is constrained by Equation (33). Self-discharging rate (heat loss) of thermal storage tank ( $\tau_{TST}$ ) has been incorporated in HCS of previous time step ( $Q_{HCS}^{PRE}(t)$ ) as given by Equation (33) [37]. Equation (34) defines the allowable range for HCS of thermal storage tank. Finally, Equation (35) implies that charging and discharging rates of thermal storage will be bounded by 0 and 1:

$$0 \leq Q_{CH}^h(t) \leq \left( \frac{\max[Q_{TST}^h] - Q_{HCS}^{PRE}(t) \cdot Q^{CAP}}{\eta_{CR}^h} \right), \forall t \quad (30)$$

$$0 \leq Q_{DISCH}^h(t) \leq \left( \left( Q_{HCS}^{PRE}(t) \cdot Q^{CAP} - \min[Q_{TST}^h] \right) \right) \cdot \eta_{DISCH}^h, \forall t \quad (31)$$

$$HCS(t) = Q_{HCS}^{PRE}(t) \cdot Q^{CAP} + Q_{CR}^h(t) \cdot \eta_{CR}^h - \frac{Q_{DISCH}^h(t)}{\eta_{DISCH}^h}, \forall t \quad (32)$$

$$Q_{HCS}^{PRE}(t) \leq \begin{cases} Q_{HPL}^{INIT} \cdot (1 - \tau_{TST}) & \text{if } t = 1 \\ HCS(t-1) \cdot (1 - \tau_{TST}) & \text{else} \end{cases}, \forall t \quad (33)$$

$$\min[HCS] \leq HCS(t) \leq \max[HCS], \forall t \quad (34)$$

$$0 \leq \eta_{CH}^h, \eta_{DISCH}^h \leq 1, \forall t \quad (35)$$

### 3.6. Energy Carrying Capacity Constraints

Both current-carrying electric lines and thermal energy carrying pipelines have finite capacities. Constraints related to the energy carrying capacity of each medium (electric line or thermal pipeline) are given by following equations:

$$0 \leq Q_{CH_m}^h(t), Q_{DISCH_m}^h(t) \leq Q_m^{HCAP}, \forall m, t \quad (36)$$

$$0 \leq P_{BUY_m}^e(t), P_{SELL_m}^e(t) \leq P_m^{CAP}, \forall m, t \quad (37)$$

$$0 \leq (Q_{ADC_m}^c(t) + Q_{EHP_m}^c(t)) \leq Q_m^{CCAP}, \forall m, t \quad (38)$$

$$0 \leq P_{BUY_L}^e(t), P_{SELL_L}^e(t) \leq P_L^{CAP}, \forall t \quad (39)$$

The amount of thermal energy charged/discharged to/from the thermal storage tank should not exceed the capacity of the pipe connecting the  $m$ th BMG with the thermal storage tank as given by Equation (36). Similarly, the amount of electricity traded with the utility grid should not exceed the capacity of line connecting the  $m$ th BMG with the utility grid as given by Equation (37). The total amount of cooling energy received by  $m$ th BMG is limited by the capacity of the pipe connecting cooling energy sources with the given BMG as shown in Equation (38). Finally, the amount of electricity traded between the utility grid and EEN is constrained by Equation (39).

## 4. Numerical Simulations

In order to illustrate the effectiveness of the proposed strategy, three BMGs have been considered in this study. Each BMG has a small CHP along with electricity, heating, and cooling demands. Demands (both thermal and electricity) of each BMG are different for different seasons of the year. The demand (electricity, heating, and cooling) patterns have been collected from the year-round data of the three selected buildings in Seoul (Korea). Building 1 (BMG1) is a residential building, building 2 (BMG2) is a commercial complex, and building 3 (BMG3) is an industrial building. In this study, representative days from the two extreme seasons have been selected to validate the feasibility of the developed model for the daily operation of building multi-microgrid systems. Demand patterns of 15 July and 15 January have been selected as representative demands for summer and winter

seasons, respectively. All the numerical simulations have been coded in C++ in Microsoft visual studio environment using CPLEX 12.3 [38].

#### 4.1. Input Data

Demands of individual BMGs, time-of-use price signals, and generation costs of CHPs are illustrated in this section. Figures 3 and 4 show the electricity, heating, and cooling demand profiles of BMGs in summer and winter seasons, respectively. It can be observed that cooling demand is dominant in summer season while heating demand is dominant in the winter season. The electricity demand profile of each BMG follows the same pattern with different magnitudes in both the seasons. Being a commercial building, the change in electricity demand in BMG2 is very prominent in working and non-working hours. While the difference is comparatively lesser in BMG3, some equipment needs to operate all the time. Time-of-use price signals (buying and selling prices) for trading electricity with the utility grid along with per-unit generation costs of CHPs are shown in Figure 5. Time-of-use market price signals are taken from [39] and are scaled. Large CHP is the most expensive unit and small CHP1 is the least expensive unit.

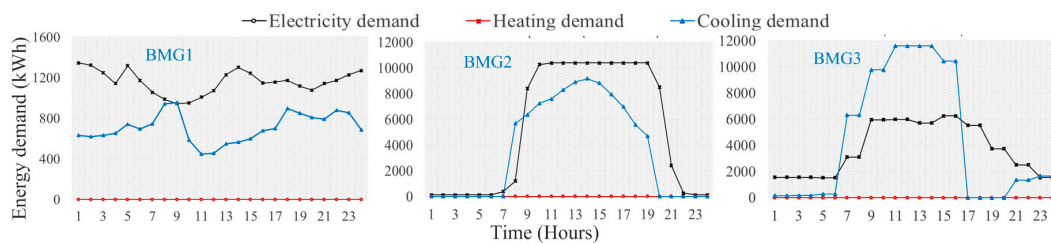


Figure 3. Electricity, heating, and cooling demand profiles of BMGs in summer season.

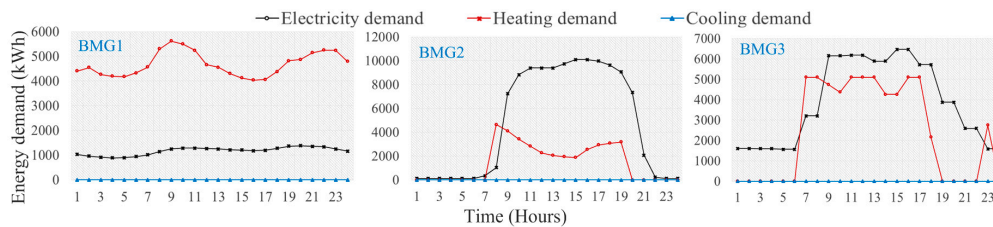


Figure 4. Electricity, heating, and cooling demand profiles of BMGs in winter season.

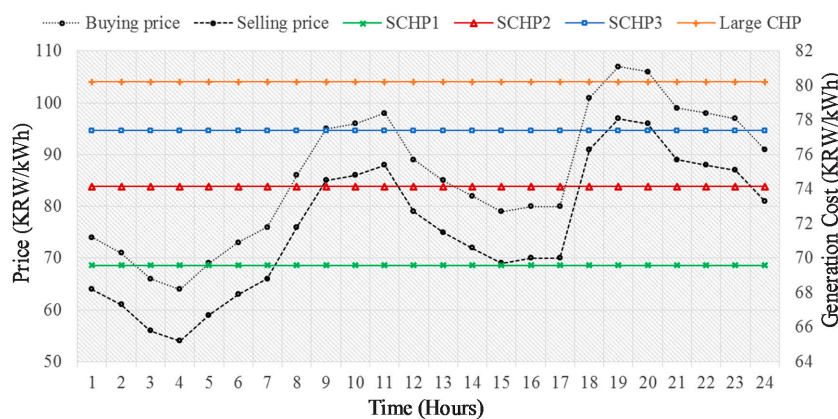


Figure 5. Time-of-use market price signals with generation costs of CHPs.

Energy generation ranges of different equipment used in the building multi-microgrid system with their energy efficiency ratings (where applicable) are tabulated in Table 1. Prices for trading heat

energy between BMGs and EEN are tabulated in Table 2. Different prices are determined for summer and winter seasons for each BMG in 2015 and are taken as input parameters. The trading prices for the summer and winter seasons are the same. Heat to power ratios and overall efficiencies of gas turbine, fuel cell, and large CHP are taken from [40], and those of Stirling engine from [41] and are tabulated in Table 2. A loss of 4% has been taken as a thermal energy (heat and cooling) loss for thermal pipes and a loss of 2% for electric lines.

**Table 1.** Energy generation limits and energy efficiency ratings.

Parameters	EHP	ADC	Stirling Engine	Fuel Cell	Gas Turbine	Large CHP
Minimum (kW)	0	0	0	0	0	0
Maximum (kW)	200,000	170,000	1000	1000	1000	200,000
Energy Efficiency Rating (%)	400	60	-	-	-	-
Overall efficiency (%)	-	-	92	65	70	75

**Table 2.** Season-wise heat trading prices of BMGs and heat to power ratios of CHPs.

Season	Selling Price (KRW)			Buying Price (KRW)			Heat to Power Ratio			
	BMG1	BMG2	BMG3	BMG1	BMG2	BMG3	Stirling Engine	Fuel Cell	Gas Turbine	Large CHP
Summer	63.47	44.40	53.90	78.47	59.40	59	3.5	1.0	1.8	1.25
Winter	74	72	63	90	67	78	3.5	1.0	1.8	1.25

#### 4.2. Scheduling of Building Multi-Microgrid System in Summer Season

The collective (electricity, heating, and cooling) demand is at its peak in the summer season. 15 July represents the summer season in this study. The demand for electricity in BMG1 has increased in summer season due to severe environmental conditions as shown in Figure 6a. In order to fulfill the electricity demand, BMG1 has bought electricity from the utility grid in all the intervals of time except time intervals 8–11. Due to the absence of heat demand in the summer season, all the generated heat has been sold to the EEN as depicted in Figure 6b. Cooling demand can be seen in all time intervals of the selected day in BMG1. However, the magnitude of cooling demand is lower in BMG1 as compared to other two BMGs. The optimization algorithm constraints the EEN to equally share the cooling energy generated by both ADC and EHP. Due to lower operation cost, ADC will be utilized first, and remaining cooling demand will be fulfilled by using EHP. Owing to the lower cooling demand of BMG1, only ADC has been utilized by EEN as shown in Figure 6c. Electric power loss due to the trading of electricity with the utility grid and thermal loss due to the trading of thermal energy with EEN are shown in Figure 6d.

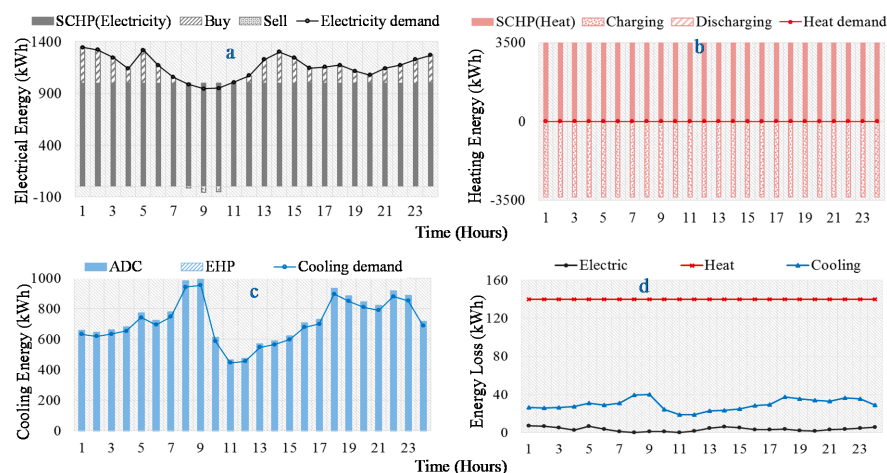


**Figure 6.** Energy balancing of BMG1 in summer season: (a) electrical energy; (b) heating energy; (c) cooling energy; and (d) energy loss.

BMG2 being a commercial complex, the difference in electricity demand increases drastically in the working hours. Figure 7a shows that in peak demand intervals, i.e., time intervals 9–21, electricity demand has been fulfilled by buying electricity from the utility grid. However, in the non-working intervals, electricity has been sold to the utility grid by BMG2 after fulfilling local demand. It can be observed from Figure 7a that small CHP2 has generated maximum electricity even when its generation cost is higher than the buying price, i.e., intervals 1–6. This behavior is due to the ability of the BMG2 to sell the heat energy to EEN. If only electricity-trading prices were considered, BMG2 would produce minimum electricity in time intervals 1–6. In the non-operating hours, the surplus amount of electricity has been sold to the utility grid. Similar to BMG1, there is no heat demand in BMG2 during the summer season as shown by Figure 7b. Selling of heat energy to EEN benefits the building multi-microgrid system in two folds. Firstly, individual BMGs can increase their profit by selling heat energy. Secondly, EEN can use the accumulated heat to generate cooling energy and sell it back to the BMGs, which increases the profit of EEN. The cooling demand has significantly increased during the working hours of BMG2. Due to the limited capacity of ADC, only ADC is not sufficient to fulfill the cooling demand of BMG2 in the operating hours. ADC has been primarily used and remaining cooling demand has been fulfilled by using EHP as depicted in Figure 7c. The magnitude of cooling demand is at its peak in the noon hours for BMG2. It can be observed from Figure 8d that the amount of cooling energy losses dominates other two losses and it follows the cooling load profile.

The magnitude of the electricity demand of BMG3 has increased significantly in the summer season. Due to higher magnitude of electricity demand, BMG3 has bought electricity from the utility grid in all hours of the day as shown in Figure 8a. Similar to other two BMGs, BMG3 also has no heat demand in the summer season. All heat produced by small CHP3 has been sold to EEN, which will be used by EEN to generate cooling energy through ADC. An abrupt increased in the cooling demand can be observed in the operating hours of BMG3 from Figure 8c.

Due to higher magnitude of cooling demand in time intervals 7–17, only ADC is not able to suffice the entire cooling demand of BMG3. The amount of cooling demand that is beyond the capacity of ADC has been generated through EHP by EEN. Similar to BMG2, the peak cooling demand of BMG3 was also in the noon hours as shown in Figure 8c. Due to the higher amount of cooling load, more cooling energy is bought from the EEN and cooling losses dominate other losses, as shown in Figure 8d.

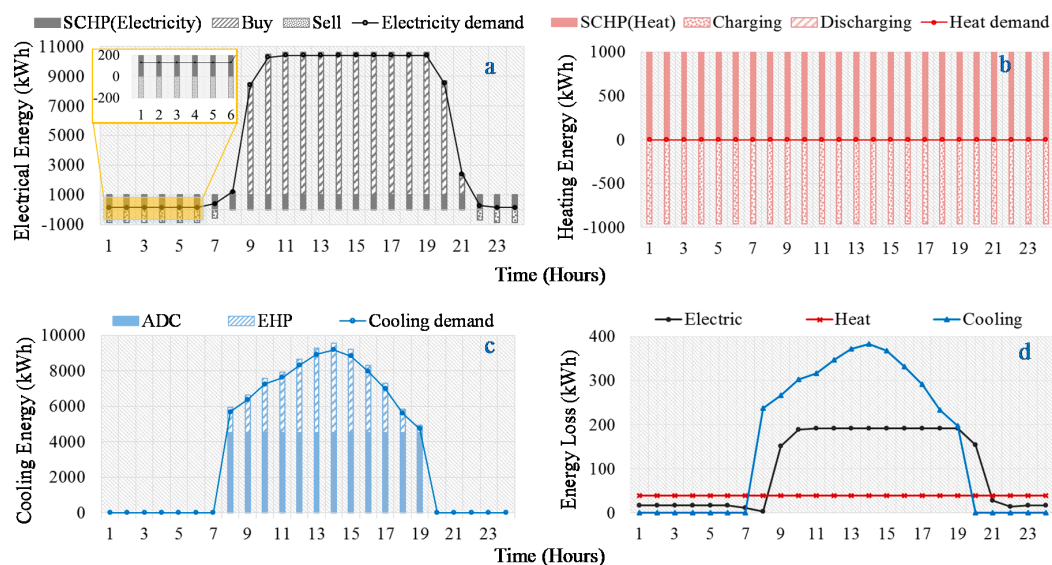


**Figure 7.** Energy balancing of BMG2 in summer season: (a) electrical energy; (b) heating energy; (c) cooling energy; and (d) energy loss.

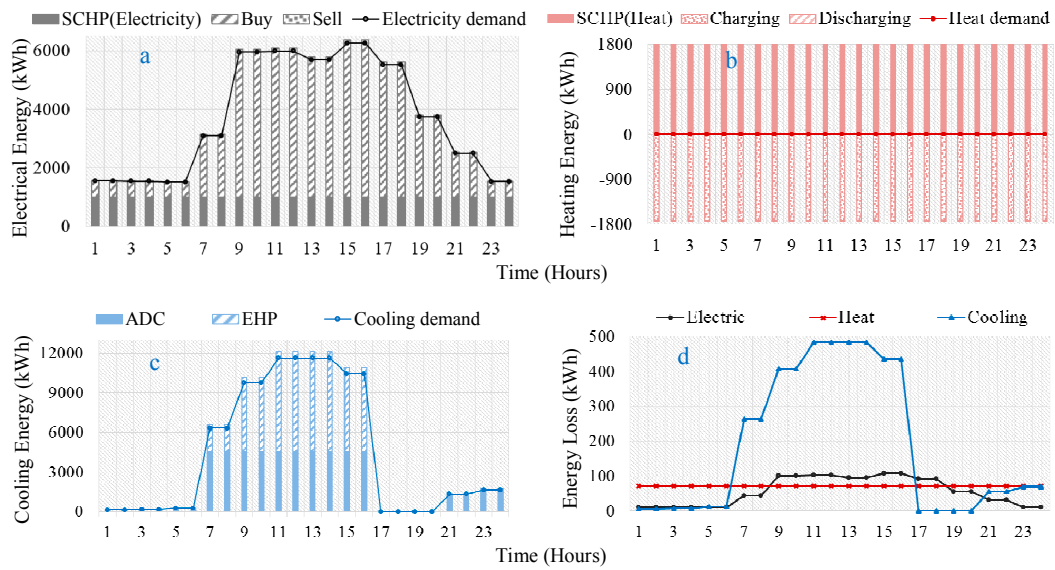


**Figure 8.** Energy balancing of BMG3 in summer season: (a) electrical energy; (b) heating energy; (c) cooling energy; and (d) energy loss.

The generation of electricity by large CHP in EEN depends on the market trading price. Therefore, in time intervals 9–11 and 18–24, it generated to its fullest as shown in Figure 9a. During these time intervals, the generation cost of large CHP is lesser than selling price as depicted in Figure 5. EHP is considered as an electricity load by the EEN. Therefore, in time intervals 12–14 the generation amount of large CHP has been increased by an amount equal to the requirement of EHP as shown in Figure 9a. It can be observed from Figure 5 that the generation cost of large CHP is sandwiched between the buying and selling prices from the utility grid. Therefore, it is more profitable to increase the generation of large CHP instead of buying from the utility grid during time intervals 12–14. The cooling and heating losses of the EEN, shown in Figure 9c, are equal to the accumulative losses of individual BMGs. The electrical loss is due to trading of power between EEN and the utility grid. It can be observed that during the summer season due to higher magnitude of the cooling load, more cooling energy is bought by BMGs from the EEN. This resulted in a dominant cooling energy loss while the heating loss of the network remained constant due to the absence of heating loads. Finally, electric power loss is a function of the amount of power traded by the entire network with the utility grid.

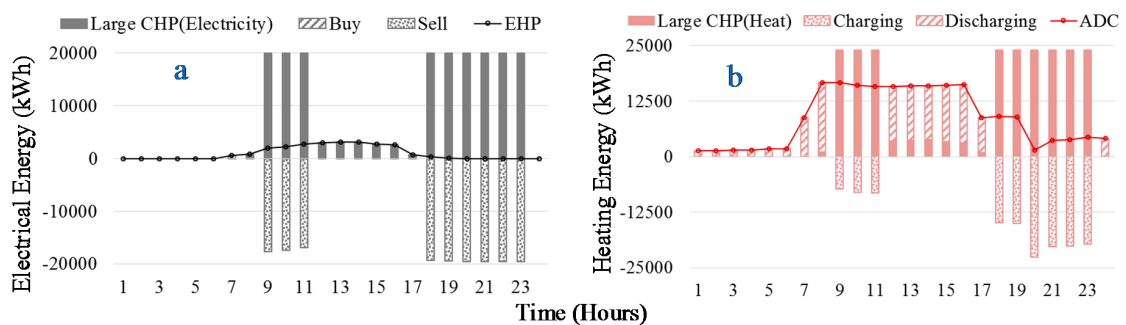


**Figure 9.** Cont.

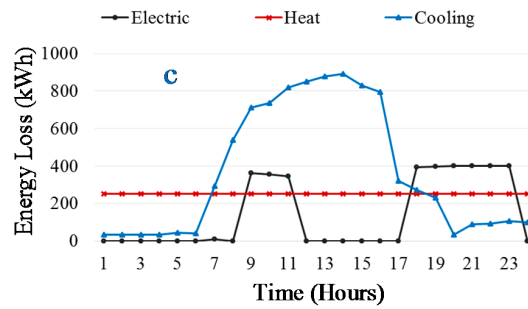


**Figure 9.** Energy balancing of EEN in summer season: (a) electrical energy; (b) heating energy; and (c) energy loss.

### 4.3. Scheduling of Building Multi-Microgrid System in Winter Season

January 15 has been taken as the representative day of the winter season in this study. Due to severe environmental conditions, energy demand in winter has increased drastically. It can be observed from Figures 10–13 that apart from electricity demand, heat demand has also increased in all the BMGs in the winter season. Apart from early morning hours, i.e., time intervals 1–7 electricity has been bought from the utility grid by BMG1 to fulfill its electricity demand. BMG1 is electrically self-sufficient in time interval 7 only, as depicted in Figure 10a. Being a residential BMG, the peak heat demand has been observed in time intervals 8–10 with a semi-peak at time intervals 21–23. However, during the entire day, heat has been bought from EEN to fulfill the local heat demand as depicted in Figure 10b. There was no cooling demand in BMG1 in the winter season, therefore; cooling energy balancing was not required for BMG1 in the winter season. Figure 10d shows the electric and thermal power losses of the BMG1 during different hours of the day.

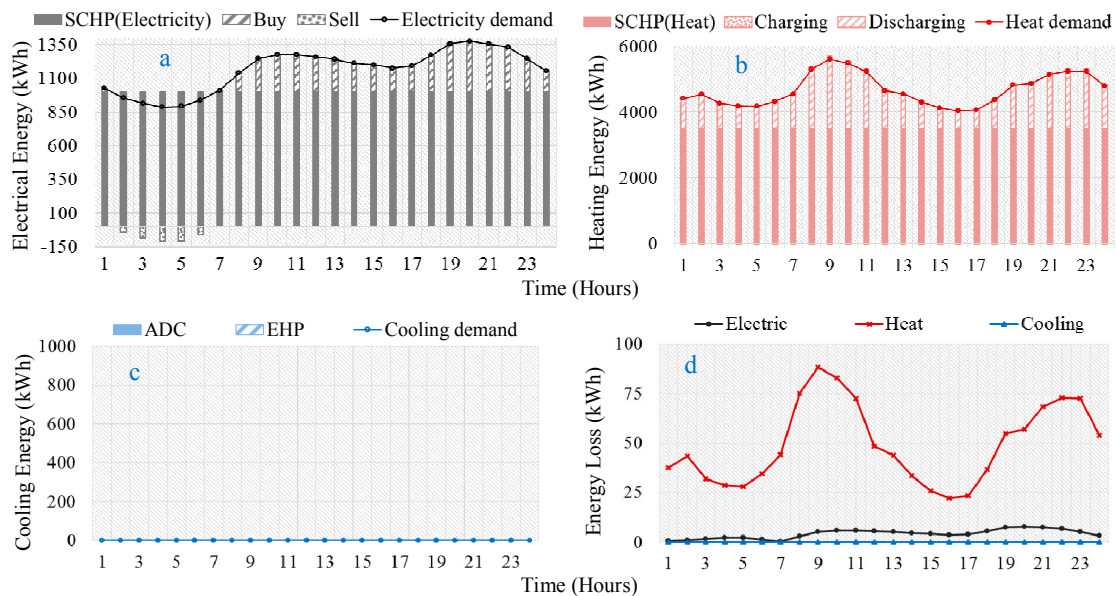


**Figure 10.** Energy balancing of BMG1 in winter season: (a) electrical energy; (b) heating energy; (c) cooling energy; and (d) energy loss.

BMG2 being a commercial complex, the general trend of electricity demand in winter season is similar to that of the summer season. The electricity demand is negligible during non-office hours, i.e., 1–8 and 20–24. Therefore, during these time intervals, the excess of electricity generated by small CHP2 has been sold to the utility grid as shown in Figure 11a. During office hours, a major portion of electricity demand has been fulfilled by buying electricity from the utility grid.

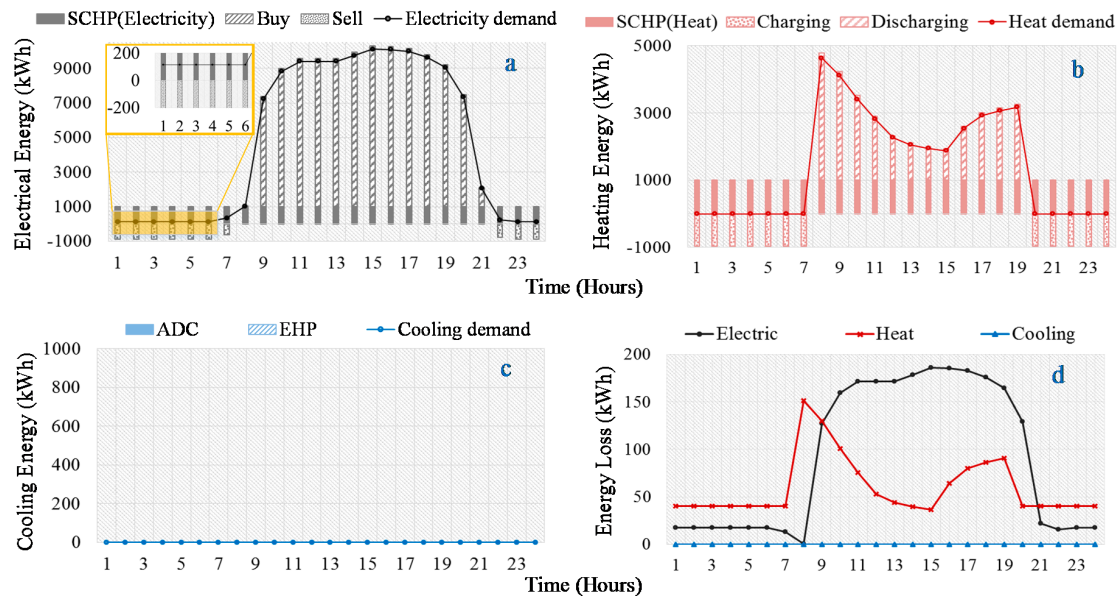


**Figure 11.** Energy balancing of BMG2 in winter season: (a) electrical energy; (b) heating energy; (c) cooling energy; and (d) energy loss.

Similar to electricity demand, heat demand has also significantly increased in the office hours. Due to the absence of heat demand in non-working hours, all the heat generated during those time intervals has been sold to the EEN as depicted in Figure 11b. Additionally, the peak heat demand was observed in the early morning hours with another peak at early afternoon hours. During all the working hours, however, heat has been bought from EEN to fulfill the heat energy demand of BMG2. Similar to BMG1, BMG2 also has no cooling demand in the winter season. It can be observed from Figure 12d that electric power loss is a function of the amount of power traded with the utility grid and thermal energy loss is a function of the amount of heat energy traded with the EEN.

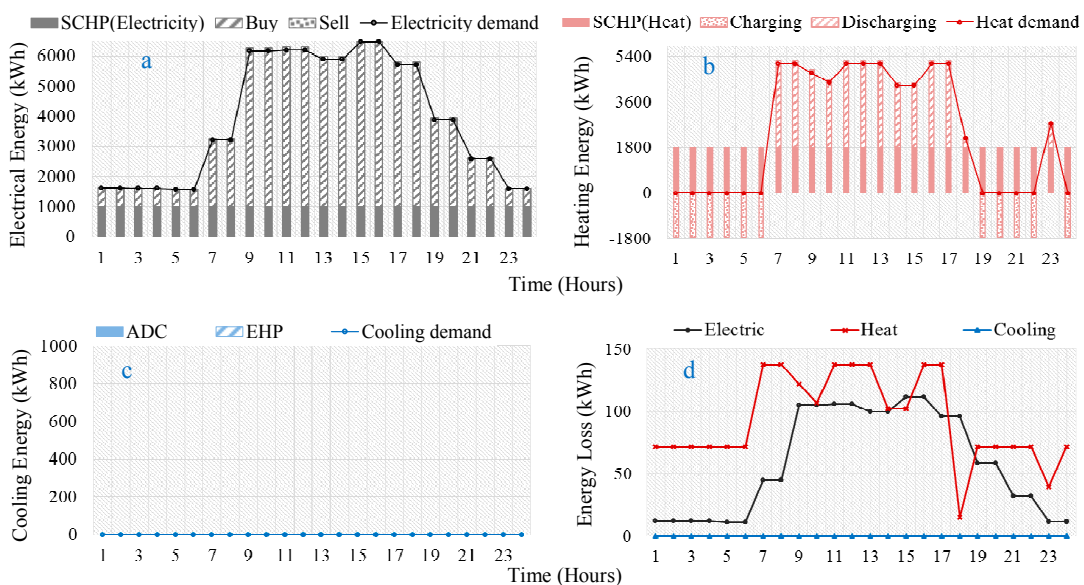


**Figure 12.** Energy balancing of BMG3 in winter season: (a) electrical energy; (b) heating energy; (c) cooling energy; and (d) energy loss.

Due to the presence of identical equipment and similar work pattern in BMG3, the electricity demand of BMG3 is similar throughout all the seasons of the year. Electricity has been bought from

the utility grid in all the time intervals of the selected day to fulfill the electricity demand of BMG3 as depicted in Figure 12a.

The heat demand is negligible or absent in the non-operating hours. Therefore, heat generated during the non-operating hours has been sold to the EEN. Due to this ability of BMG to sell the heat energy, small CHP3 has always generated maximum power in all the time intervals, even though in some time intervals the buying price of electricity was lower than the generation cost of small CHP3. As depicted by Figure 12b, the heat energy demand in the operating hours of BMG3 is irregular due to the difference in activities of workers in different time intervals of the day. Similar to BMG2, the power loss and thermal energy loss patterns follow the amount of energy traded with the utility grid and the EEN, respectively.

Due to the absence of cooling demand in all the BMGs, ADC and EHP have not been operated by EEN. ADC is treated as the thermal load and EHP as the electric load of EEN. Therefore, the electricity and thermal demands (EHP and ADC, respectively) for EEN are zero throughout the day. Large CHP has been operated by only considering the market selling price. Large CHP has been fully operated in time intervals 9–11 and 18–24 due to higher selling price during those time intervals as shown in Figure 13a. All the generated electricity has been sold to the utility grid to increase the profit of EEN. Similarly, all the heat generated due to the generation of electricity has been charged to heat storage tank as shown in Figure 13b. The stored heat energy has been used for fulfilling the heat demand of BMGs. Due to the absence of cooling load, cooling energy has not been traded in the winter season and hence cooling energy loss is zero for the entire network. Due to the trading of a large amount of power during time intervals 9–12 and 18–23, lot of line losses occurred in the EEN during these time intervals. Finally, heat loss of the network can be seen as an accumulated loss of individual BMGs, as shown in Figure 13c.

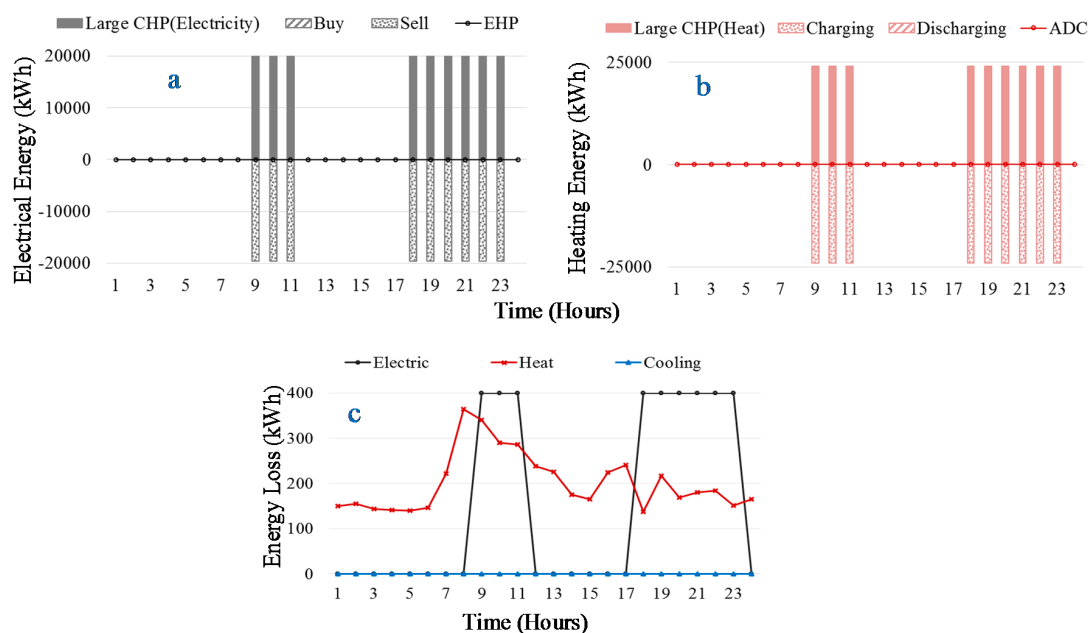


**Figure 13.** Energy balancing of EEN in winter season: (a) electrical energy; (b) heating energy; and (c) energy loss.

#### 4.4. Scheduling Behavior of CHPs and Comparison in Different Seasons

After analyzing the operation behavior of different CHPs in different seasons of the year, following conclusions can be deduced:

- Balancing of electrical, heat, and cooling energies is coupled and generation of CHPs may be increased/decreased due to increase/decrease in demand for one or more energy types.

- Due to the ability of BMGs to sell the heat energy to EEN, the generation patterns have been totally changed. If only electricity trading prices have been considered small CHPs had generated:
  - (a) Minimum electricity in those time intervals where generation cost is higher than the market selling price.
  - (b) Maximum electricity in those time intervals where generation cost is lower than market buying price.
  - (c) Electricity equal to the local demand in those time intervals where generation cost is between selling price and buying prices.
- Large CHP being the part of EEN, is not able to sell the heat energy directly to EEN. Therefore, electricity generated by large CHP is controlled by market price signals.
- EEN has increased the generation amount of large CHP in those time intervals where cooling and/or heat demand of BMGs are out of the capacity of local small CHPs and thermal energy stored in the thermal storage tank.
- There is a significant change in energy demands in BMG2 and BMG3 due to high-energy consumption in working hours. While the energy demand in BMG1 is comparatively flat due to the presence of energy demand in all the time intervals of the day.

The performance of the proposed energy management strategy is compared against the performance of a conventional energy management approach. In the conventional approach, each BMG fulfills its energy demands by using its local elements. Extra heat is wasted after fulfilling local thermal energy demands while a boiler and an EHP are used by each BMG for fulfilling its peak load demand. In the proposed strategy, an EEN is introduced for fulfilling the thermal demands of the BMGs where, BMGs can trade thermal energy with the EEN. Additionally, due to the presence of cooling network, individual BMGs do not contain local cooling devices. It can be observed from Table 3 that thermal losses of the entire network are reduced by 84.36% in the summer season and by 28.74% in the winter season. The thermal energy loss of the proposed strategy is due to pipeline losses for transporting energy from the EEN to BMGs and vice versa. The daily operation cost of the conventional approach and the proposed strategy for each entity of the network is shown in Table 4. It can be observed from Table 4 that, the proposed strategy has reduced the daily operation cost of the entire network by 45.45% for the summer season and by 38.48% for the winter season.

**Table 3.** Thermal energy loss in conventional approach and the proposed strategy in different seasons.

Entity	Conventional Approach (kWh)		Proposed Strategy (kWh)		Reduction (%)	
	Summer	Winter	Summer	Winter	Summer	Winter
BMG1	84,000	0.00	4067.08	1180.2	95.16	−100
BMG2	24,000	12,000	4603.5	1431.38	80.82	88.07
BMG3	43,200	1670	6174.25	2243.791	85.71	−34.36
EEN	-	-	8796.83	4855.37	−100	−100
Entire Network	151,200	13,670	23641.67	9740.86	84.36	28.74

**Table 4.** Operation cost of the conventional approach and the proposed strategy in different seasons.

Entity	Conventional Approach (KRW)		Proposed Strategy (KRW)		Reduction (%)	
	Summer	Winter	Summer	Winter	Summer	Winter
BMG1	2,721,430	5,479,592	−1,711,354	4,380,839	59.02	20.05
BMG2	15,724,555	13,537,269	14,802,795	11,829,877	5.86	12.61
BMG3	12,310,664	12,093,229	9,734,640	10,178,609	20.93	15.83
EEN	-	-	−6,049,457	−7,248,858	100	100
Entire Network	30,756,648	31,110,090	16,776,624	19,140,468	45.45	38.48

## 5. Conclusions

New thermal energy management aspects such as a bilateral heat trading between the energy supplier and the customers, the so-called energy prosumer concept, are proposed in this study by using the thermal storage tank along with the conventional district heating and cooling systems. It has been observed that all the small CHPs and the EEN have compromised their operating schedules for maximizing the benefit of individual BMGs and the EEN. A mathematical model has been developed for minimizing the daily operation cost of the EEN while fulfilling the CCHP energy demands of the BMGs. Scheduling of resources for all the three forms of energies, i.e., electricity, heat, and cooling energy in the three selected buildings has been carried out for the two extreme seasons of the year. In terms of thermal energy losses, the proposed strategy has reduced the daily thermal losses of the entire network by 84.36% during the summer season. In the winter season, the daily thermal losses of the network have been reduced by 28.74%. This higher reduction in summer season is due to utilization of waste heat of BMGs by the EEN for generation of cooling energy, which was wasted by BMGs in the conventional approach. In terms of operation cost, the proposed energy management strategy can benefit both the EEN owners and the BMG owners. The daily operation cost of BMG1, BMG2, and BMG3 has been reduced by 59.02%, 5.86%, and 20.93%, respectively in the summer season. During the summer season, EEN has gained a profit of 604,9457 KRW by trading thermal energy with BMGs and electricity with the utility grid. The daily operation cost of the entire network has been reduced by 45.45% during the summer season. Similarly, during the winter season, the operation cost of BMG1, BMG2, and BMG3 has been reduced by 20.05%, 12.61%, and 15.83%, respectively. The profit of EEN has increased to 7,248,858 KRW in the winter season due to the selling of more thermal energy to BMGs and electricity to the utility grid. The daily operation cost of the entire network has been reduced by 38.48% during the winter season. This reduction in operation cost and thermal energy losses have been achieved owing to the utilization of more energy efficient components by BMGs and the EEN due to networking.

**Acknowledgments:** This work was supported by In-house Research and Development Program of the Korea Institute of Energy Research (KIER) (B7-2413-03).

**Author Contributions:** Yong-Hoon Im and Jae-Yong Lee conceived and designed the experiments; Van-Hai Bui performed the experiments; Hak-Man Kim proofread and analyzed the data; and Akhtar Hussain wrote the paper.

**Conflicts of Interest:** The authors declare no conflict of interest.

## Nomenclature

### Identifiers and Binary Variables

$t$	Index of time, running from 1 to $T$ .
$m$	Index of microgrids, running from 1 to $M$ .
$k$	Identifier of small CHP type, running from 1 to $K$ .
$e, h, c$	Identifiers for electrical, heat, and cooling energies, respectively.
$s, L, E$	Identifiers for small CHP, large CHP, and EEN, respectively.
$\eta$	Heat to power ratio/energy efficiency rating identifier [%].
$\tau$	Self-discharging loss identifier for thermal storage tank [%].
₩	South Korean Won.
$x_{k,m}$	Indicator for small CHP type in microgrid $m$ .
$u_{k,m}(t), u_L(t), u_a(t)$	Commitment status of $k$ th type small CHP, large CHP, and ADC, respectively at $t$ .
$y_{k,m}(t), y_L(t), y_a(t)$	Start-up indicator of $k$ th type small CHP, large CHP, and ADC, respectively at $t$ .

### Variables and Constants

$E^{EEN}(t)$	Amount of energy generated by EEN at $t$ [kWh].
$C_{EEN}(t)$	Generation cost for $E^{EEN}(t)$ [₩].
$P_{LOAD_m}^e(t)$	Electricity demand of $BMG\ m$ at $t$ [kWh].
$C_{k,m}^s, C_{CHP}^L$	Per unit generation cost of small CHP $k$ and large CHP, respectively [₩/kWh].

$P_{k,m}^s(t)$	Amount of electricity generated by small CHP $k$ in $BMG$ $m$ at $t$ [kWh].
$PR_{BUY}^e(t), PR_{SELL}^e(t)$	Price for buying/selling electricity from/to utility grid at $t$ [€/kWh].
$P_{BUY_m}^e(t), P_{SELL_m}^e(t)$	Amount of electricity bought from and sold to the utility grid by $BMG$ $m$ at $t$ [kWh].
$P_{CHP}^L(t)$	Amount of electricity generated by large CHP at $t$ [kWh].
$P_{BUY_L}^e(t), P_{SELL_L}^e(t)$	Amount of electricity bought from and sold to the utility grid by EEN at $t$ [kWh].
$P_{BUY}^e(t), P_{SELL}^e(t)$	Total amount of electricity bought from sold to the utility grid by building multi-microgrid system at $t$ [kWh].
$P_{EHP}^e(t)$	Amount of electricity consumed by EHP at $t$ [kWh].
$SUC_{k,m}^s(t), SUC_{CHP}^L(t)$	Start-up cost for small CHP $k$ and large CHP, respectively at $t$ [€].
$Q_{LOAD_m}^h(t), Q_{LOAD_m}^c(t)$	Heating and cooling demand of $BMG$ $m$ at $t$ [kWh].
$PR_{BUY_m}^h(t), PR_{SELL_m}^h(t)$	Price for buying/selling heat energy from/to EEN by $BMG$ $m$ at $t$ [€/kWh].
$Q_{CH_m}^h(t), Q_{DISCH_m}^h(t)$	Amount of heat charged/discharged to/from the storage tank by $BMG$ $m$ at $t$ [kWh].
$Q_{k,m}^h(t)$	Amount of heat generated by small CHP $k$ in $BMG$ $m$ at $t$ [kWh].
$Q_L^h(t)$	Amount of heat generated by large CHP at $t$ [kWh].
$Q_{W_m}^h(t), Q_{EW}^h(t)$	Amount of heat wasted by $BMG$ $m$ and EEN at $t$ [kWh].
$Q_W^h(t)$	Total amount of heat wasted by building multi-microgrid system at $t$ [kWh].
$Q_{LCH}^h(t)$	Amount of heat charged to thermal storage tank by large CHP at $t$ [kWh].
$PR_{SELL_m}^c(t)$	Price for buying cooling energy from EEN by $BMG$ $m$ at $t$ [€/kWh].
$Q_{ADC}^c(t), Q_{EHP}^c(t)$	Amount of cooling energy generated by ADC and EHP at $t$ [kWh].
$Q_{ADC_m}^c(t), Q_{EHP_m}^c(t)$	Amount of cooling energy used by $BMG$ $m$ from ADC and EHP at $t$ [kWh].
$Q_{TST}^h(t)$	Amount of heat stored in thermal storage tank at $t$ [kWh].
$HCS(t)$	Heat content of storage of thermal storage tank at $t$ [%].
$Q_{HCS}^{PRE}(t)$	HCS of the thermal storage tank at $t - 1$ [%].
$Q_{HPL}^{INIT}$	Amount of heat present in the thermal storage tank at the beginning of day [kWh].
$Q^{CAP}$	Capacity of thermal storage tank [kWh].
$P_m^{CAP}$	Capacity of the line connecting $BMG$ $m$ with utility grid [kWh].
$P_E^{CAP}$	Capacity of the line connecting EEN with utility grid [kWh].
$Q_m^{HCAP}$	Capacity of heat pipe connecting $BMG$ $m$ with thermal storage tank [kWh].
$Q_m^{CCAP}$	Capacity of cooling pipe connecting $BMG$ $m$ with cooling sources [kWh].
$\eta_{k,m}, \eta_L$	Electricity to heat conversion efficiencies of small and large CHPs [%].
$\eta_{ADC}, \eta_{EHP}$	Energy efficiency ratings of ADC and EHP [%].
$\eta_{CR}^h, \eta_{DISCH}^h, \tau_{TSt}$	Charging, discharging, and self-discharging efficiencies of thermal storage tank [%].
$P_{loss_m}^s, Q_{loss_m}^h, Q_{loss_m}^c$	Power loss of line, heat loss of pipe, and cooling loss of pipe of $m$ th microgrid [%].
$P_{loss}^L, Q_{loss}^h$	Power loss of electric line and heat loss of pipe of EEN [%].

## References

1. Nikos, H.; Asano, H.; Iravani, R.; Marnay, C. Microgrids: An overview of ongoing research, development, and demonstration projects. *IEEE Power Energy Mag.* **2007**, *5*, 78–94.
2. Marnay, C.; Chatzivasileiadis, S.; Abbey, C.; Iravani, R.; Appen, J. Microgrid evolution roadmap. In Proceedings of the IEEE International Symposium Smart Electric Distribution Systems and Technologies, Vienna, Austria, 8–11 September 2015.
3. Cho, H.; Smith, A.D.; Mago, P. Combined cooling, heating and power: A review of performance improvement and optimization. *Appl. Energy* **2014**, *136*, 168–185. [[CrossRef](#)]
4. Hussain, A.; Arif, S.M.; Aslam, M. Emerging renewable and sustainable energy technologies: State of the art. *Renew. Sustain. Energy Rev.* **2017**, *71*, 12–28. [[CrossRef](#)]
5. Carpenter, J.; Mago, P.J.; Luck, R.; Cho, H. Passive energy management through increased thermal capacitance. *Energy Build.* **2014**, *75*, 465–471. [[CrossRef](#)]

6. Oh, S.D.; Yoo, Y.; Song, J.; Song, S.J.; Jang, H.N.; Kim, K.; Kwak, H.Y. A cost-effective method for integration of new and renewable energy systems in public buildings in Korea. *Energy Build.* **2014**, *74*, 120–131. [[CrossRef](#)]
7. Wouters, C.; Fraga, E.S.; James, A.M. An energy integrated, multi-microgrid, MILP (mixed-integer linear programming) approach for residential distributed energy system planning—A South Australian case-study. *Energy* **2015**, *85*, 30–44. [[CrossRef](#)]
8. Thangavelu, S.R.; Nutkani, I.U.; Hwee, C.M.; Myat, A.; Khambadkone, A. Integrated electrical and thermal grid facility-testing of future microgrid technologies. *Energies* **2015**, *8*, 10082–10105. [[CrossRef](#)]
9. Gu, C.; Xie, D.; Sun, J.; Wang, X.; Ai, Q. Optimal operation of combined heat and power system based on forecasted energy prices in real-time markets. *Energies* **2015**, *8*, 14330–14345. [[CrossRef](#)]
10. Li, Z.; Wu, W.; Shahidehpour, M.; Wang, J.; Zhang, B. Combined heat and power dispatch considering pipeline energy storage of district heating network. *IEEE Trans. Sustain. Energy* **2016**, *7*, 12–22. [[CrossRef](#)]
11. Li, Z.; Wu, W.; Wang, J.; Zhang, B.; Zheng, T. Transmission-Constrained unit commitment considering combined electricity and district heating networks. *IEEE Trans. Sustain. Energy* **2016**, *7*, 480–492. [[CrossRef](#)]
12. Zhang, X.; Karady, G.G.; Piratla, K.R.; Ariaratnam, S.T. Network capacity assessment of combined heat and power-based distributed generation in urban energy infrastructures. *IEEE Trans. Smart Grid* **2013**, *4*, 2131–2138. [[CrossRef](#)]
13. Negendahl, K.; Nielsen, T.R. Building energy optimization in the early design stages: A simplified method. *Energy Build.* **2015**, *105*, 88–99. [[CrossRef](#)]
14. Perea, E.; Ruiz, N.; Cobelo, I.; Lizuain, Z.; Carrascal, A. A novel optimization algorithm for efficient economic dispatch of combined heat and power devices. *Energy Build.* **2016**, *111*, 507–514. [[CrossRef](#)]
15. Song, N.O.; Lee, J.H.; Kim, H.M. Optimal electric and heat energy management of multi-microgrids with sequentially-coordinated operations. *Energies* **2016**, *9*, 473. [[CrossRef](#)]
16. Bracco, S.; Delfino, F.; Pampararo, F.; Robba, M.; Rossi, M. A dynamic optimization-based architecture for polygeneration microgrids with tri-generation, renewables, storage systems and electrical vehicles. *Energy Convers. Manag.* **2015**, *96*, 511–520. [[CrossRef](#)]
17. Ascione, F.; Canelli, M.; De Masi, R.F.; Sasso, M.; Vanoli, G.P. Combined cooling, heating and power for small urban districts: An Italian case-study. *Appl. Therm. Eng.* **2014**, *71*, 705–713. [[CrossRef](#)]
18. Guo, L.; Liu, W.; Cai, J.; Hong, B.; Wang, C. A two-stage optimal planning and design method for combined cooling, heat and power microgrid system. *Energy Convers. Manag.* **2013**, *74*, 433–445. [[CrossRef](#)]
19. Hussain, A.; Arif, S.M.; Aslam, M.; Shah, S.D.A. Optimal siting and sizing of tri-generation equipment for developing an autonomous community microgrid considering uncertainties. *Sustain. Cities Soc.* **2017**, *32*, 318–330. [[CrossRef](#)]
20. Gu, W.; Wu, Z.; Bo, R.; Liu, W.; Zhou, G.; Chen, W.; Wu, Z. Modeling, planning and optimal energy management of combined cooling, heating and power microgrid: A review. *Int. J. Electr. Power Energy Syst.* **2014**, *54*, 26–37. [[CrossRef](#)]
21. Wu, T.; Mai, W.; Qin, M.; Zhang, C.; Li, J.; Chung, C.Y. Optimal operation of combined cooling heat and power microgrid with PEVs. In Proceedings of the IEEE PowerTech, Eindhoven, The Netherlands, 29 June–2 July 2015.
22. Hakimi, S.M.; Moghaddas-Tafreshi, S.M.; Hassanzadehfard, H.; Taylor, G.A.; Alamuti, M.M. Optimization of a reliable combined cooling, heat and power microgrid system. In Proceedings of the IEEE Industrial Electronics Society, Vienna, Austria, 10–13 November 2013.
23. Gao, P.; Dai, Y.; Tong, Y.; Dong, P. Energy matching and optimization analysis of waste to energy CCHP (combined cooling, heating and power) system with exergy and energy level. *Energy* **2015**, *79*, 522–535. [[CrossRef](#)]
24. Colmenar-Santos, A.; Rosales-Asensio, E.; Borge-Diez, D.; Collado-Fernández, E. Evaluation of the cost of using power plant reject heat in low-temperature district heating and cooling networks. *Appl. Energy* **2016**, *162*, 892–907. [[CrossRef](#)]
25. Wang, J.; Wu, J.; Zheng, C. Analysis of tri-generation system in combined cooling and heating mode. *Energy Build.* **2014**, *72*, 353–360. [[CrossRef](#)]
26. Gupta, S.; Jain, P.; Yeoh, W.; Ranade, S.; Pontelli, E. Solving customer-driven microgrid optimization problems as DCOPs. In Proceedings of the Distributed Constraint Reasoning Workshop, Beijing, China, 4 August 2013; pp. 45–59.

27. Mamidi, S.K.; Chang, Y.H.; Maheswaran, R. Adaptive learning agents for sustainable building energy management. In Proceedings of the 2012 AAAI Spring Symposium Series, Stanford, CA, USA, 26–28 March 2012; pp. 46–53.
28. Gilan, S.S.; Dilkina, B. Sustainable building design: A challenge at the intersection of machine learning and design optimization. In Proceedings of the Workshops at the Twenty-Ninth AAAI Conference on Artificial Intelligence, Austin, TX, USA, 25–26 January 2015; pp. 101–106.
29. Fioretto, F.; Yeoh, W.; Pontell, E. A multiagent system approach to scheduling devices in smart homes. In Proceedings of the AAAI Conference on Artificial Intelligence, San Francisco, CA, USA, 4–9 February 2017.
30. Tabakhi, A.M.; Fioretto, F.; Yeoh, W. A Preliminary Study on Preference Elicitation in DCOPs for Scheduling Devices in Smart Buildings. Available online: <https://www.cs.nmsu.edu/~ffiorett/papers/files/mpref-2016.pdf,2017> 2017 (accessed on 6 June 2017).
31. Kluegel, W.; Iqbal, M.A.; Fioretto, F.; Yeoh, W.; Pontelli, E. A realistic dataset for the smart home device scheduling problem for DCOPs. *arXiv* **2017**, arXiv:1702.06970.
32. Zhang, W.; Ma, Y.; Liu, W.; Ranade, S.; Luo, Y. Distributed optimal active power dispatch under constraints for smart grids. *IEEE Trans. Ind. Electr.* **2016**, *64*, 5084–5094. [[CrossRef](#)]
33. Hussain, A.; Bui, V.H.; Kim, H.M. Robust optimization-based scheduling of multi-microgrids considering uncertainties. *Energies* **2016**, *9*, 278. [[CrossRef](#)]
34. Nguyen, D.T.; Le, L.B. Optimal energy management for cooperative microgrids with renewable energy resources. In Proceedings of the IEEE International Conference on Smart Grid Communications, Vancouver, BC, Canada, 21–24 October 2013.
35. Underwood, C.; Ng, B.; Yik, F. Scheduling of multiple chillers in trigeneration plants. *Energies* **2015**, *8*, 11095–11119. [[CrossRef](#)]
36. Persson, U.; Ruehling, K.; Felsmann, C.; Crane, M.; Burzynski, R.; Wiltshire, R.; Bevilacqua, C. Toward 4th generation district heating: Experience and potential of low-temperature district heating. In Proceedings of the 14th International Symposium on District Heating and Cooling, Stockholm, Sweden, 7–9 September 2014.
37. Eames, I.W.; Evans, K.; Pickering, S. A comparative study of open and closed heat-engines for small-scale CHP applications. *Energies* **2016**, *9*, 130. [[CrossRef](#)]
38. CPLEX Division, ILOG. *IBM ILOG CPLEX V12.1: User's Manual for CPLEX 2009*; CPLEX Division, ILOG: Incline Village, NV, USA, 2009.
39. Song, N.O.; Lee, J.H.; Kim, H.M.; Im, Y.H.; Lee, J.Y. Optimal energy management of multi-microgrids with sequentially coordinated operations. *Energies* **2015**, *8*, 8371–8390. [[CrossRef](#)]
40. CHP-Cogeneration Power, Renac, Renewable Academy, Germany. Available online: [http://www.renac.de/fileadmin/renac/CHP\\_ENG\\_final.pdf](http://www.renac.de/fileadmin/renac/CHP_ENG_final.pdf) (accessed on 6 June 2017).
41. ProEcoPolyNet, Fact Sheet SOLO Stirling. Available online: <http://www.buildup.eu/sites/default/files/content/SOLO%20Stirling%20161.pdf> (accessed on 6 June 2017).

